Supporting Information

Block copolymer [(L-GluA-5-BE)-*b*-(L-AspA-4-BE)] based nanoflower capsules with thermosensitive morphology and pH-responsive drug release for cancer therapy

Chander Amgoth*[,a], Shuai Chen[a], Tirupathi Malavath[b] and Guping Tang*[,a]

[a]*Department of Chemistry, Zhejiang University, Hangzhou-310028, China*
[b]*Department of Biochemistry and Molecular Biology, Tel Aviv University, Israel*

Corresponding author: chander@uohyd.ac.in, chanderpal69@gmail.com

Characterizations Techniques

FTIR:The chemical structure and functionality of synthesized BCP of [(L-GluA-5-BE)-b-(L-AspA-4-BE)] polymers were characterized using Fourier transform infrared (FTIR, JASCO FT/IR-6600 model) spectrophotometer. The KBr pellets were used to acquire the spectra.

NMR (^{1}H and ^{13}C): The chemical structure, molecular formula and molecular weight of polymers and capsules were characterized by a Bruker DPX NMR **400 MHz (Ultra Shield^{TM}),** spectrophotometer. Powder polymer was dissolved in highly pure (98%) $CDCl_3$ and DMSO solvents at ~25 °C and poured in NMR sample tube and used for spectral analysis.

FESEM: The morphological properties like size and shape of polymer [(L-GluA-5-BE)-b-(L-AspA-4-BE)] was investigated with a Zeiss Ultra TM^{55} field emission scanning electron microscopic (FESEM) at 15 kV accelerating voltage. Samples were coated with Au-Pd.

TEM: Transmission electron microscope (Technai TEM FEI model) was used for investigating the shape, size and morphology of the samples. Carbon coated copper grids (200 mesh) has been used for the sample preparation. Polymeric samples were coated with phosphotungstic acid (PTA) to avoid sample burning at higher accelerating voltage (200 kV).

AFM: Atomic force microscopy (INTEGRA Aura model, NT-MDT, Russia) was used to investigate the surface topography through the non-contact mode of AFM. AFM tip used with of diameter ~20 nm.

DSC: Differential scanning calorimetry (DSC) experiments were performed to study the thermal and heat flow behaviour by using a TAQ200 model (Waters, Milan, Italy) DSC instrument. The samples were scanned in ~30 to 400 °C with a heating rate of ~10 °C min^{-1} in N_2 gas atmosphere.

TGA: Thermogravimetry analysis (TGA) was performed to [(L-GluA-5-BE)-b-(L-AspA-4-BE)] polymer samples to evaluate the thermal stability with a Thermo ONIX Gas lab 300 TGA with a heating rate of ~10 ^{o}C min^{-1}.

XRD: Solid state crystal structure of [(L-GluA-5-BE)-b-(L-AspA-4-BE)] polymer samples were investigated through a Bruker D8 Advance powder X-Ray diffractometer (XRD) operating in-between 10-90° (2θ) scanning range.

UV-Vis spectrophotometer: Absorbance measurements were carried out using a Perkin Elmer (Lambda-750) model UV-Vis spectrometer. Based on absorbance plots with respect to time the extent of loading and release were calculated. The calibration curve of absorbance against different concentrations of anticancer drugs such as pure Toxol were acquired at λ = 530 nm and calculated with the help of a standard plots. The calibration curve of absorbance against different concentrations of pure Toxol was acquired at ~530 nm.

Multiplate Reader: Cell based studies like cell viability and cell inhibition were investigated through the MTT assay using 96-well plates by a BioTeck Synergy H^4 multi-mode reader.

LSCM: Laser scanning confocal microscope was used to acquire the fluorescence microscopic images for drug (Toxol) loaded dendrimers and for cellular imaging before and after treatment with the help ofconfocal microscope. Fluorescence microscopy imaging experiments of the Toxol molecules loaded to NFs capsules were performed by a Zeiss LSM 700 laser scanning confocal microscope. These NFs polymeric capsules were incubated in Toxol solution for 24 hr, then it was gently washed for thrice and re-dispersed in propanol and a drop of (5µL) dispersion was taken on a glass slide. After proper drying confocal microscopy images were acquired.

Cell culture: The human epithelia cervical carcinomacancer cell line (HeLa) were grown in RPMI medium supplemented with 10% heat inactivated Fetal bovine serum (FBS), 100 IU/mL penicillin, 100 ug/mL streptomycin and 2 mM of L-glutamine and maintained in a humidified atmosphere with 5% CO_2 at ~37 °C. Cells were sub-cultured once in every three days. The anticancer drug (Toxol) was used for the treatment; Toxol was dissolved in dimethyl sulfoxide (DMSO) solvent and used to load inside the NF polymer capsules. The treatments were started with bulk number of cells, (~4 x 10^4 cells $well^{-1}$) in 60 mm petri dishes and continued with stepwise increase in the concentrations, *i.e.,* 1.0, 5.0, 10, 15, 20, and 25µg/mL. The inhibition of the HeLa cells with formulations was studied with multimode (plate) reader by using 96-well plates.

MTT assay: The MTT assay is a colorimetric method to measure the activity of enzymes in living cells to reduce MTT to formazan dyes. Upon addition to cells it gives purple colour formazan crystals. MTT assay basically used to determine cell viability, cell inhibition and cytotoxicity of potential medicines and our polymer capsules. MTT (3-(4, 5-dimethylthiazol-2-yl)-2, 5-diphenyltetrazolium bromide) is a complex chemical dye which is widely used to stain cells during treatment with DPBS buffer solution. In a 96-well plate ~4x10^4 cells per well were cultured and these wells was added with formulations with concentration of 1.0, 5.0, 10, 15, 20, and 25 µg/mL, respectively. However, 6 wells in a 96-well plate were kept blank and considered as control which means cells were as cultured. The wells contains cells were added with formulations and incubated at ~37 °C in 5% CO_2 for overnight to allow the cells to attach to the wells and interact with drug molecules which was released in media from polymer capsules. Then, calculated amount

of formulations ([(L-GluA-5-BE)-b-(L-AspA-4-BE)]) was dispersed in DMSO and then added to each well and then shaken (150 RPM for 4 min) for thorough mixing with media. Well plates were further incubated at ~37 °C in 5% CO_2 for 24 h to allow the drug/toxin to take effect on cancer cells. To those wells 15 µL of MTT solution was added and stirred with 150 RPM for ~4 min to thoroughly mixing the MTT with the media. Again plates were incubated for 24 h to allow the MTT to be metabolized with cancer cells. The excess and unwanted residue of media was dump off and plates were used to read optical density at 560 nm and subtract background at 670 nm. Optical density was directly correlated with cell quantity and obtained results were used to calculate the cell viability and inhibition.

Sputter coating: The non-conducting polymer [(L-GluA-5-BE)-b-(L-AspA-4-BE)] samples were sputter coated with metal ions (gold/Au) to get the conductivity throughout the surface of the sample. The Quorum Q150R ES model sputter coating machine has been used for the same. The coating was carried out for 3 minutes with 10 mA of current. The density of the material is 19.32 g/m^3 with gold as sputtering material. The coating rate is 1 nm/min and we obtained ~3 nm thickness of gold ions on the surface of the [(L-GluA-5-BE)-b-(L-AspA-4-BE)] sample.

EDAX:Energy dispersive X-ray spectroscopy has been used to analyze the elemental composition present in the composite of [(L-GluA-5-BE)-b-(L-AspA-4-BE)] capsules.

Tumor xenografts in nude mice

Thirty-six healthy female mice (aged 5 weeks) were housedadaptively in the specific pathogen free (SPF) animal laboratory cages with 60 -65% relative humidity, at 22 -25°C, andfree access to foodand water under12 h light/dark cycle for one week. The sorted CD133+ U87 cells were subcutaneously inoculated into the underarms of nude mice.Thereafter, the mice were randomly divided into 6 groups based on the treatment received. Tail vein injection was adopted to introduce interventions (DOX, PTX, DOX-loaded NLC, PTX-loaded NLC, or PTX and DOX-loaded NLC) into the mice from indicated group21 consecutive days. During this period, tumor volume and body weight of nude mice weremonitored and recorded. On the 28thday, mice were euthanized by intraperitoneal injection of excess barbital sodium. End-point tumor size and tumor weight were measured and the harvested tumors were fixed and prepared for histological analysis.

Statistical analysis

The data were processed using SPSS 21.0 statistical software (IBM Corp. Armonk, NY, USA). Measurement data were expressed as mean ± standard deviation. Data in compliance with normal distribution and homogeneity of variance between two groups were compared using *t*-test. Comparisons among multiple groups were conducted by one-way analysis of variance (ANOVA) with Tukey's post hoc test. A value of$p < 0.05$ indicated significant difference.All experiments were performed three times independently.

Currently,nanomedicine along with drug delivery technology exerts increasing impacts on modern medicine, which is continuouslybeing employed to development of new cancer diagnosis and treatment methods [23]. Accumulatingevidence have revealedthatNLCs can load anti-drugs to cancer cells totreat various cancers such as glioma [24].Moreover, it has recently been documented thatbothDOXand PTX contribute to glioma treatment [25, 26].Thus, the current study mainly explored the loading of PTX and DOX by NLCs and its role in GSC proliferation and apoptosis with the involvement of related molecular mechanisms. Our data mainly demonstrated that PTX-DOX-NLCs suppressedthe proliferation and accelerate apoptosis of GSCs by blocking the PI3K/Akt/mTOR signaling pathway.

Conclusion

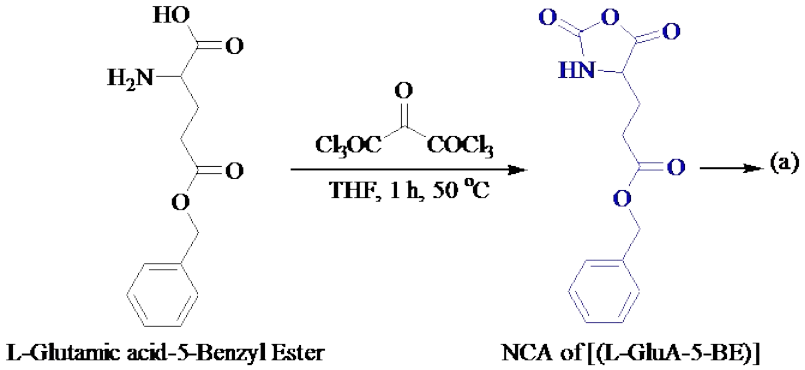

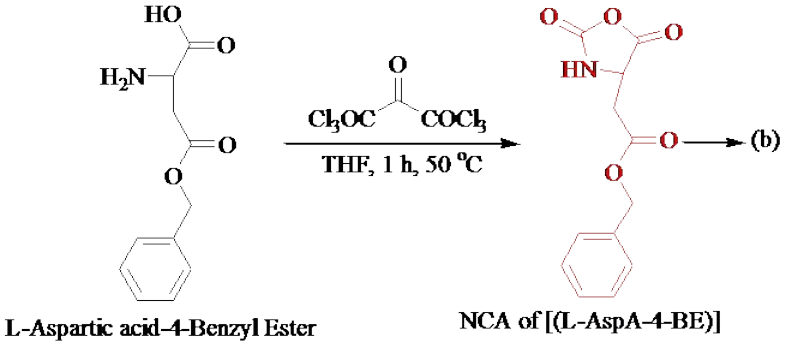

Figure:S1. Reactions involved in the conversion of cyclic anhydride followed by the oxidation with triphosgene for the final synthesis of BCP of [(L-GluA-5-BE)-b-(L-AspA-4-BE)].

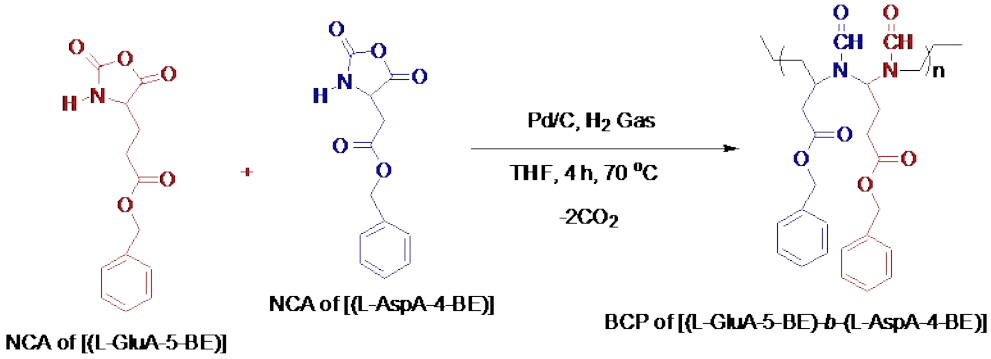

Figure: S2. Reaction corroborates the synthesis of block copolymer between cyclic anhydrides of L-GluA-5-BE and L-AspA-4-BE.

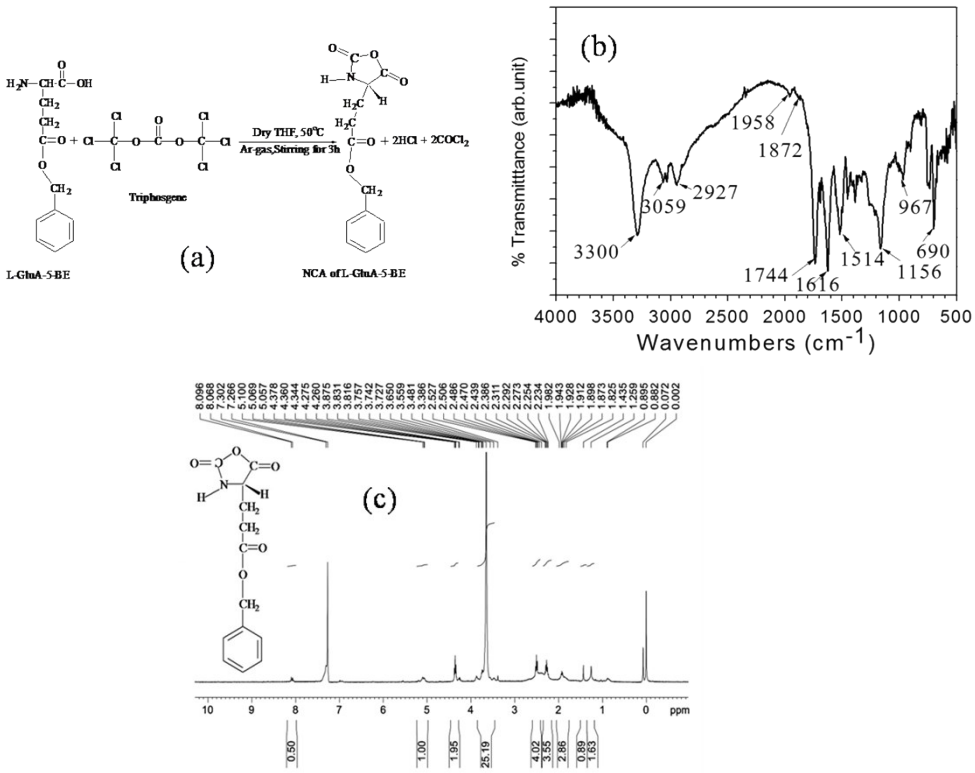

Figure: S3. Reaction (a) illustrate the oxidation of L-Glutamic acid-5-benzyl ester into cyclic anhydride of L-GluA-5-BE, plot (b) corresponds to FTIR for the synthesized NCA of L-GluA-5-BE with peak positions for corresponding functional groups, and (c) corresponds to ^{1}H-NMR o f L-GluA-5-BE.

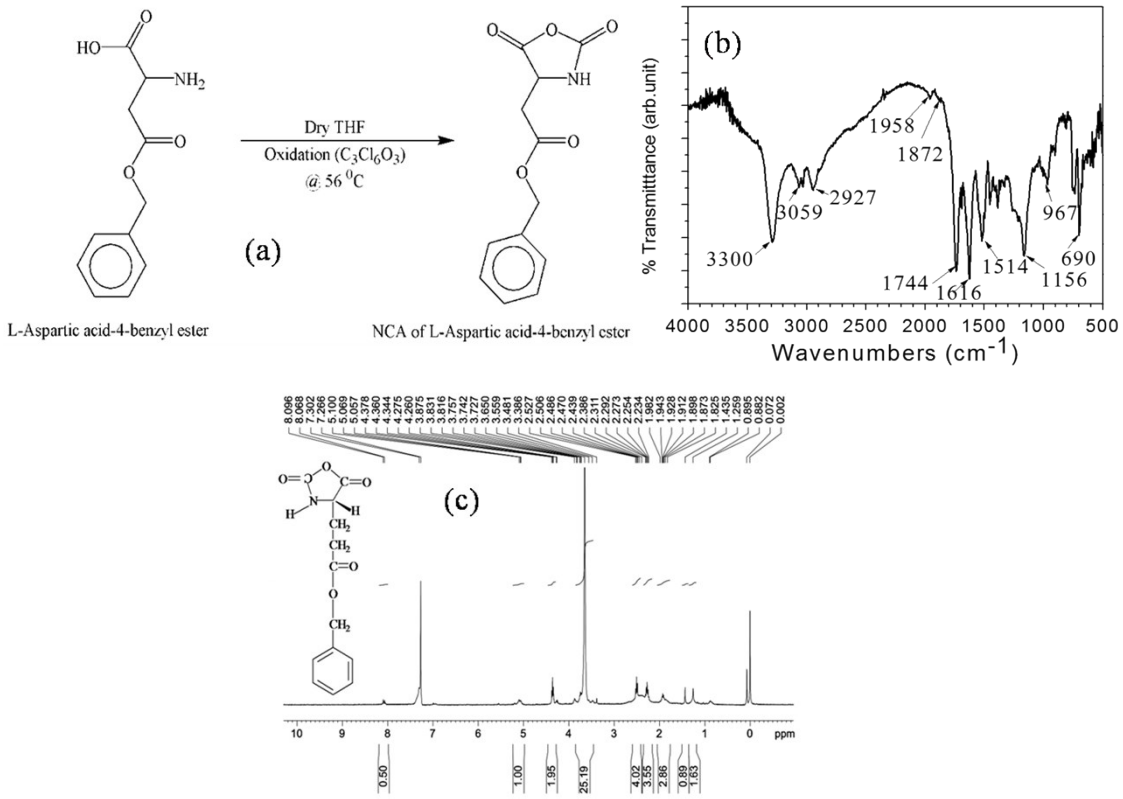

Figure: S4. Reaction (a) illustrate the oxidation of L-Aspartic acid-4-benzyl ester into cyclic anhydride of L-AspA-4-BE, plot (b) corresponds to FTIR for the synthesized NCA of L-AspA-4-BE with peak positions for corresponding functional groups, and (c) corresponds to ^{1}H-NMR o f L-AspA-4-BE.

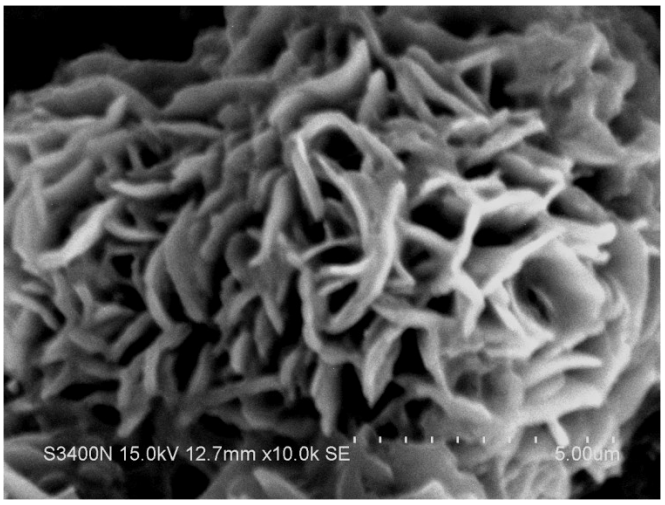

Figure: S5.SEM micrograph of NF corroborates the orientation of nanoflakes and petals on the surface of spherical polymeric capsule. The gap between the flakes and petal helps to enhance the drug loading capacity.

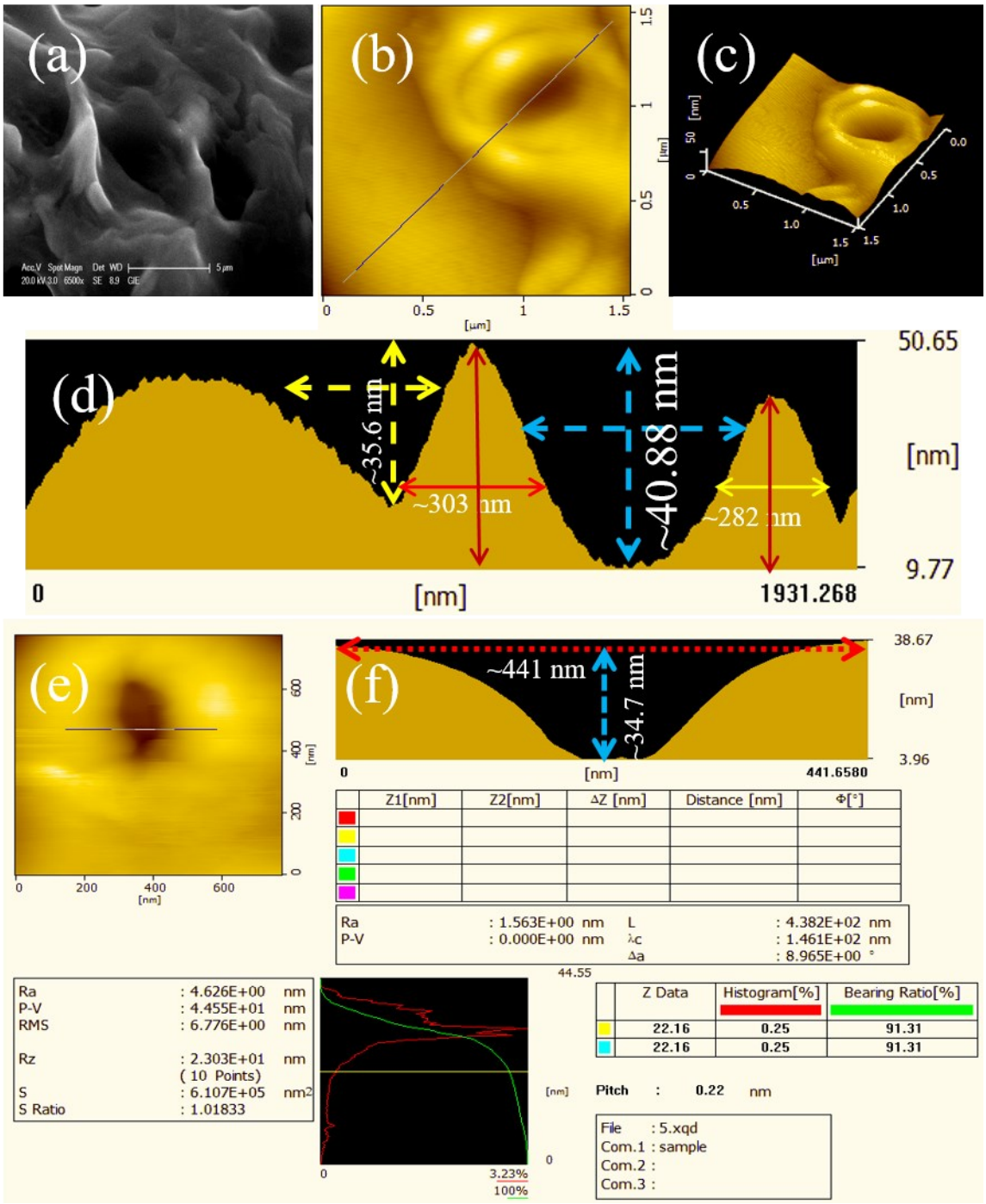

Figure: S6.SEM (a) and AFM images (b-f) depict the flake and petal thickness as well porosity throughout the surface of the capsules. From the higher magnified SEM image the thickness of the flakes can be seen with porosity but it has been measured by using the AFM characterization technique and calculated the depth and diameter of the pore along with flake thickness.

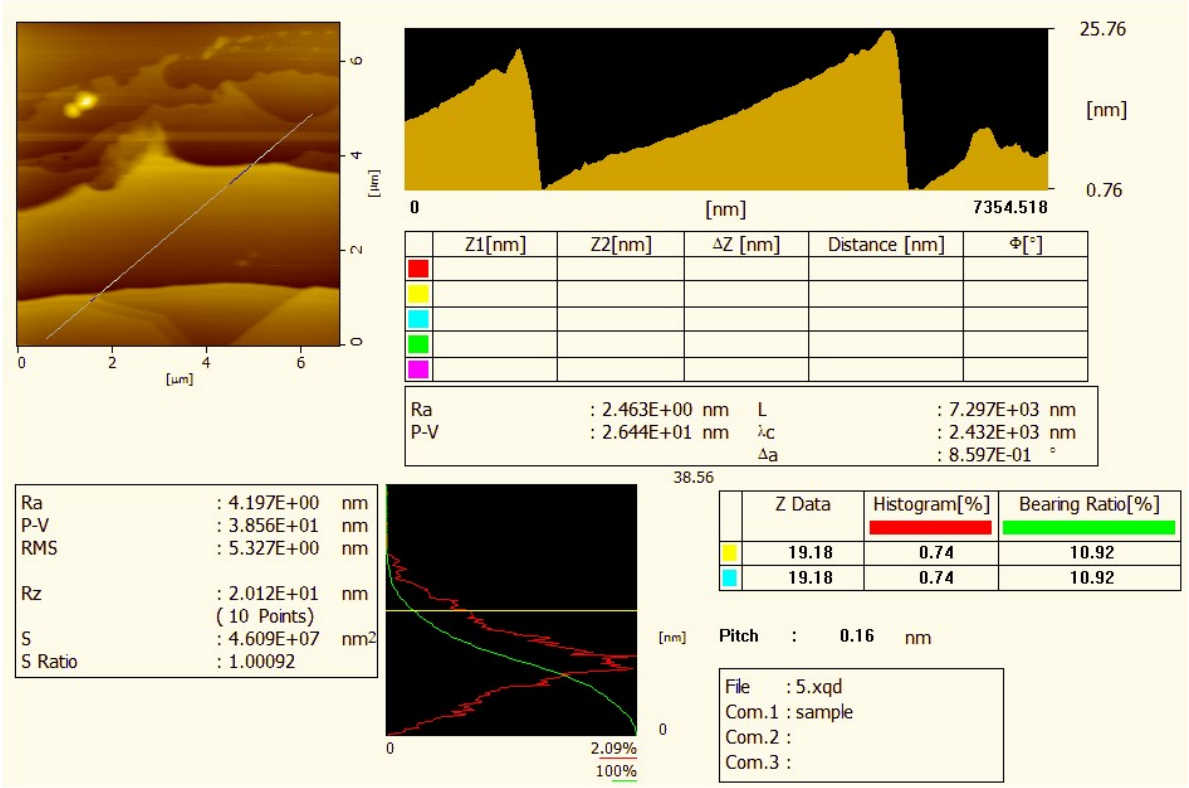

Figure: S7.AFM images depict the distribution of nanoflakes and petals throughout the surface of the particles along with rough surface and porosity. The active functional groups present in the synthesized BCP of [(L-GluA-5-BE)-b-(L-AspA-4-BE)] lead to surface functionalization.

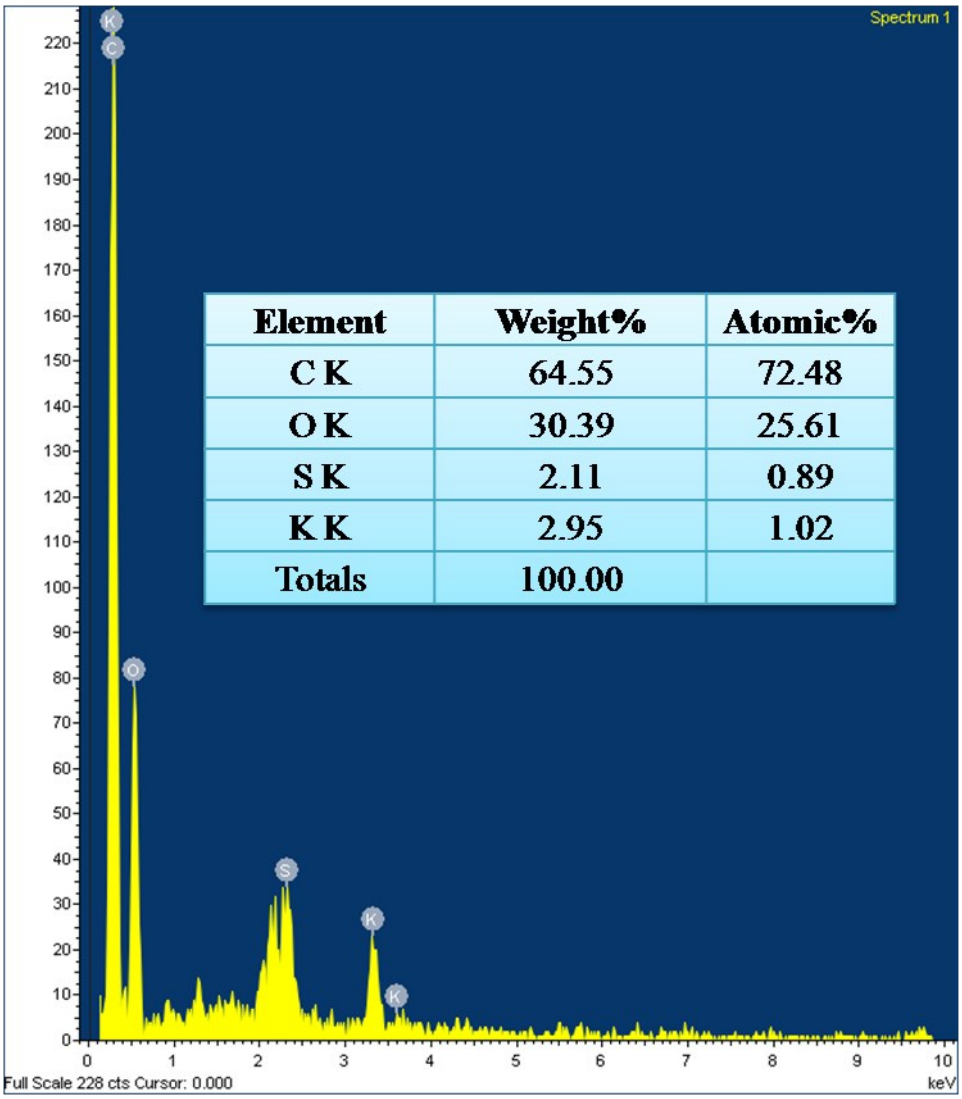

Figure: S8.EDAX plot corroborates the peak positions for carbon and oxygen atoms present in the synthesized BCP of [(L-GluA-5-BE)-b-(L-AspA-4-BE)]. The in-set table shows the presence of elements in designed nanoflowers with respect to their weight and atomic percentages.

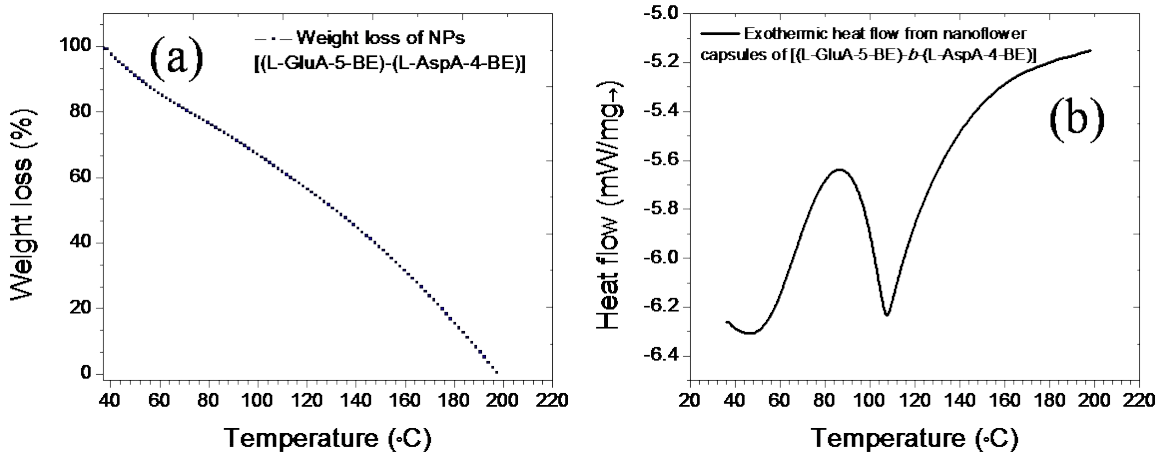

Figure: S9. Plot (a) corresponds to the TGA and shows the spontaneous degradation of nanoflower capsules with respect to increase of temperature. The plot (b) corresponds to DSC and depicts the exothermic heat flow of the nanoflower capsules.

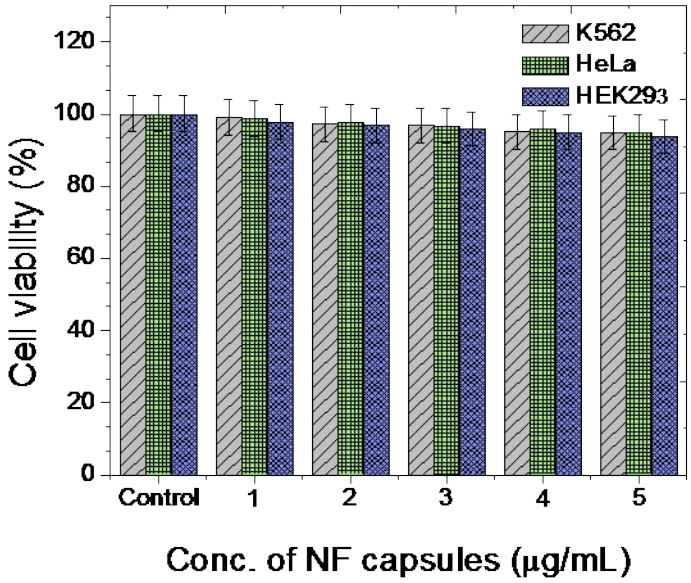

Figure: S10. Plot corroborates the cell survival rate on three different cell lines with various concentrations of synthesized nanoflower capsules.

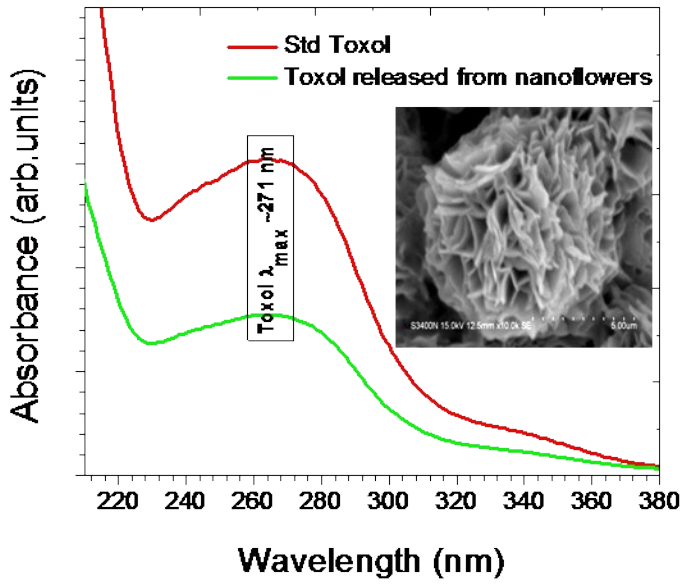

Figure: S11.UV-Vis plot corroborates the absorbance of anticancer drug/Taxol. The red curve for release/absorbance for standard Taxol and light blue curve is for Taxol released from nanoflowers.

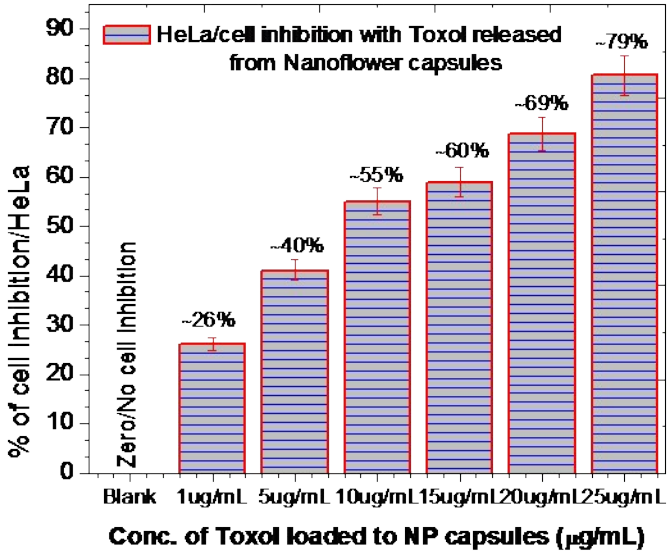

Figure: S12. Cell inhibition for the nanoformulations [(Nanoflower capsules)-(Drug/Taxol)]. HeLa cells were used for the cell based studies and obtained MTT assay data used to plot the bar graphs which shows the cell inhibition with respect to increase of concentration of Taxol.

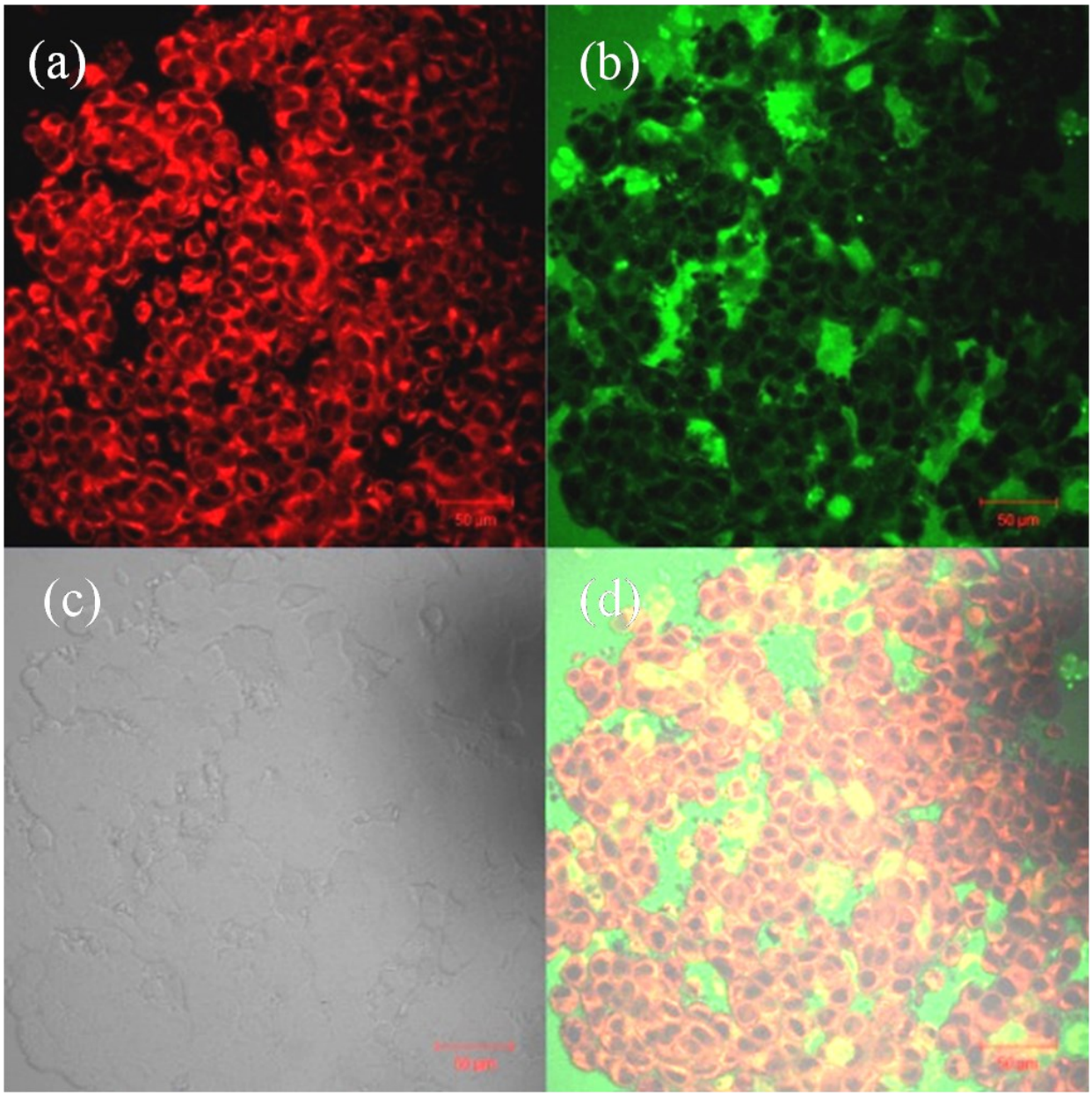

Figure: S13.LSCM images of HeLa cells treated with developed nanoformulations [(Nanoflower capsules)-(Drug/Taxol)]. After 24 hr treatment cells were stained with red fluorescent dye Rho-B (a) and green fluorescent dye FITC (b) followed by their bright field image (c) and merge of (a, b, c). The scale bar is 50 µm.

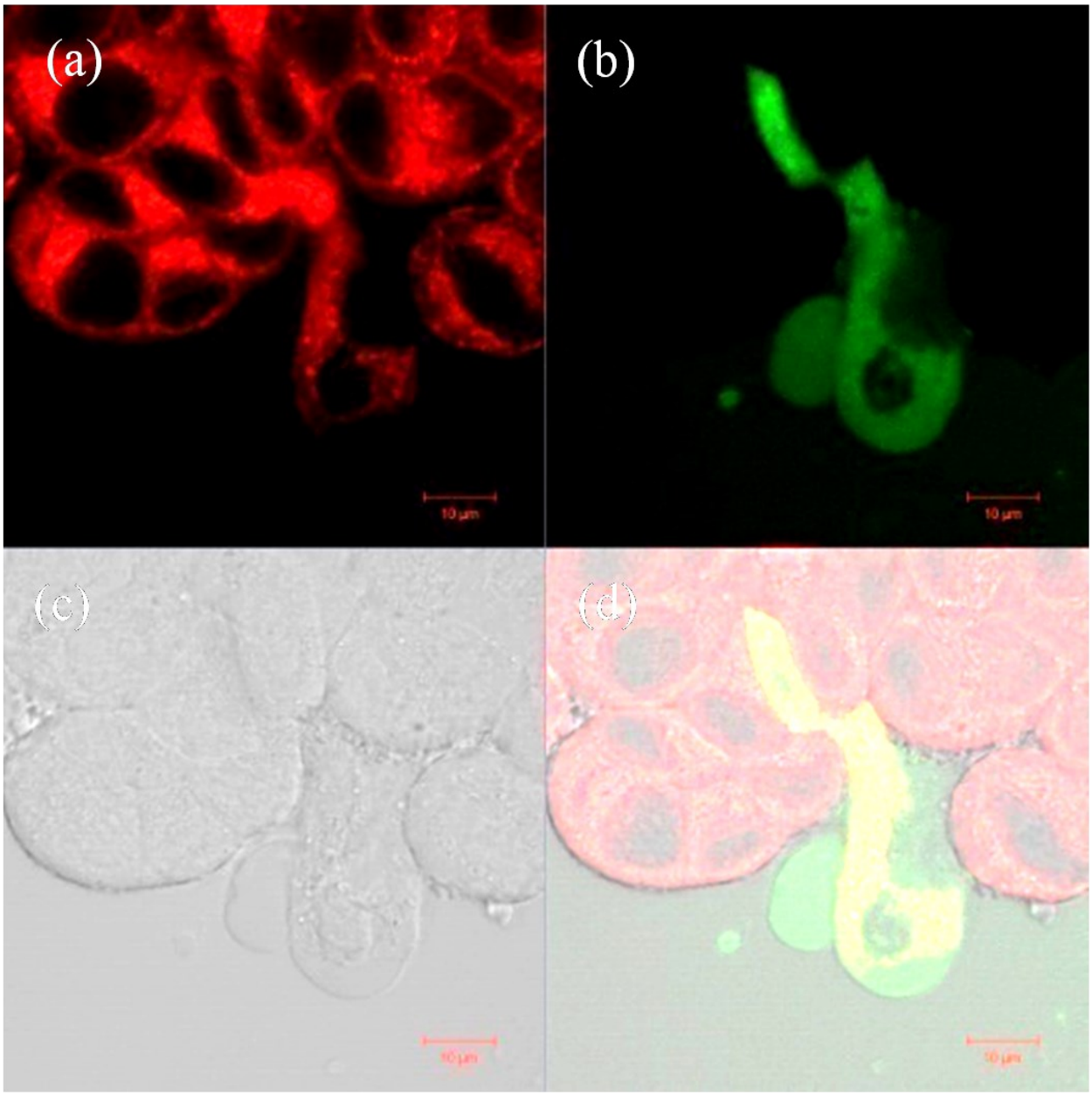

Figure: S14.LSCM images of HeLa cells treated with developed nanoformulations [(Nanoflower capsules)-(Drug/Toxol)]. After 24 hr treatment cells were stained with red fluorescent dye Rho-B (a) and green fluorescent dye FITC (b) followed by their bright field image (c) and merge of (a, b, c). The scale bar is 10 µm.

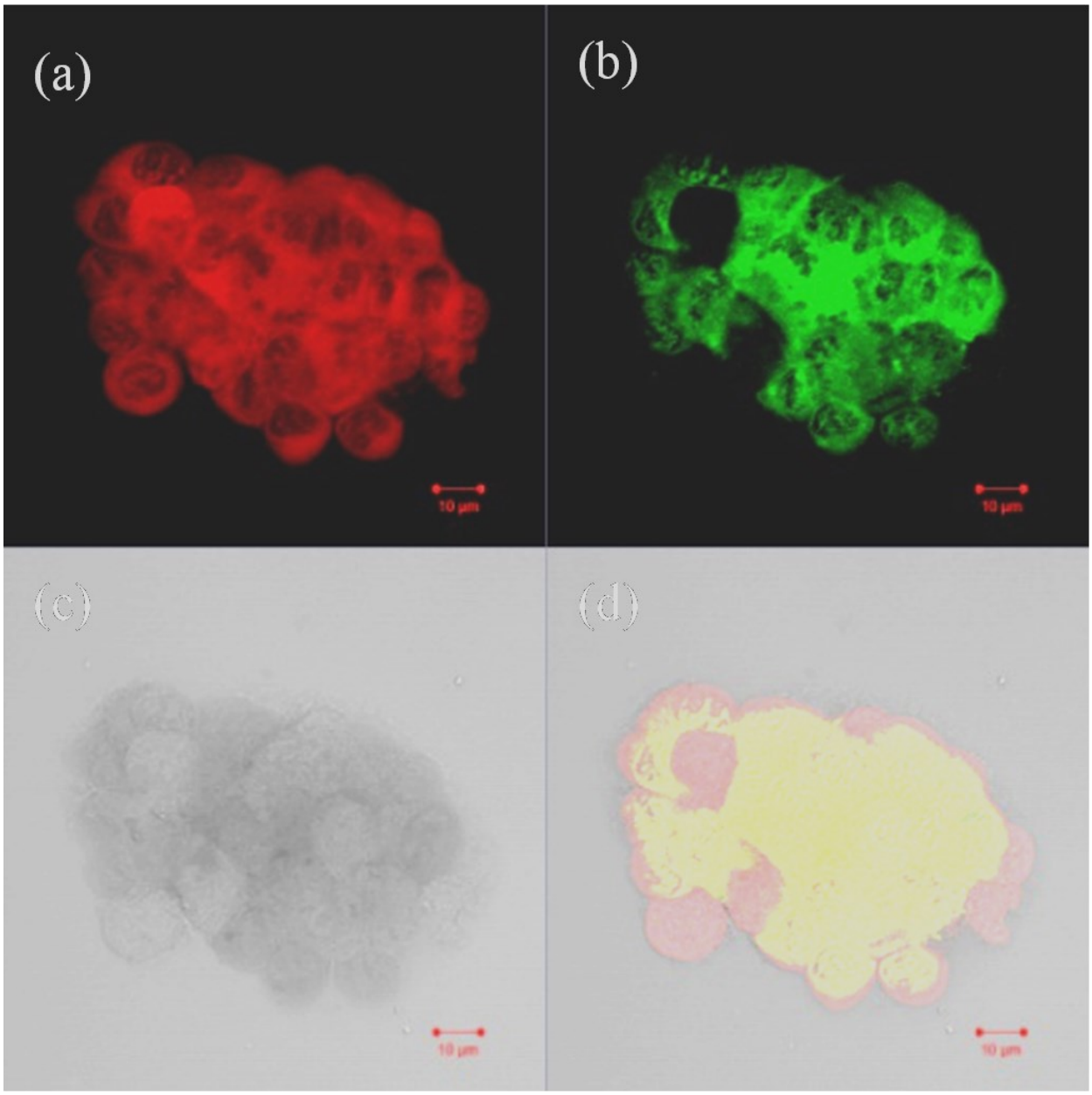

Figure: S15.LSCM images of HeLa cells treated with developed nanoformulations [(Nanoflower capsules)-(Drug/Taxol)]. After 24 hr treatment cells were stained with red fluorescent dye Rho-B (a) and green fluorescent dye FITC (b) followed by their bright field image (c) and merge of (a, b, c). The scale bar is 10 µm.

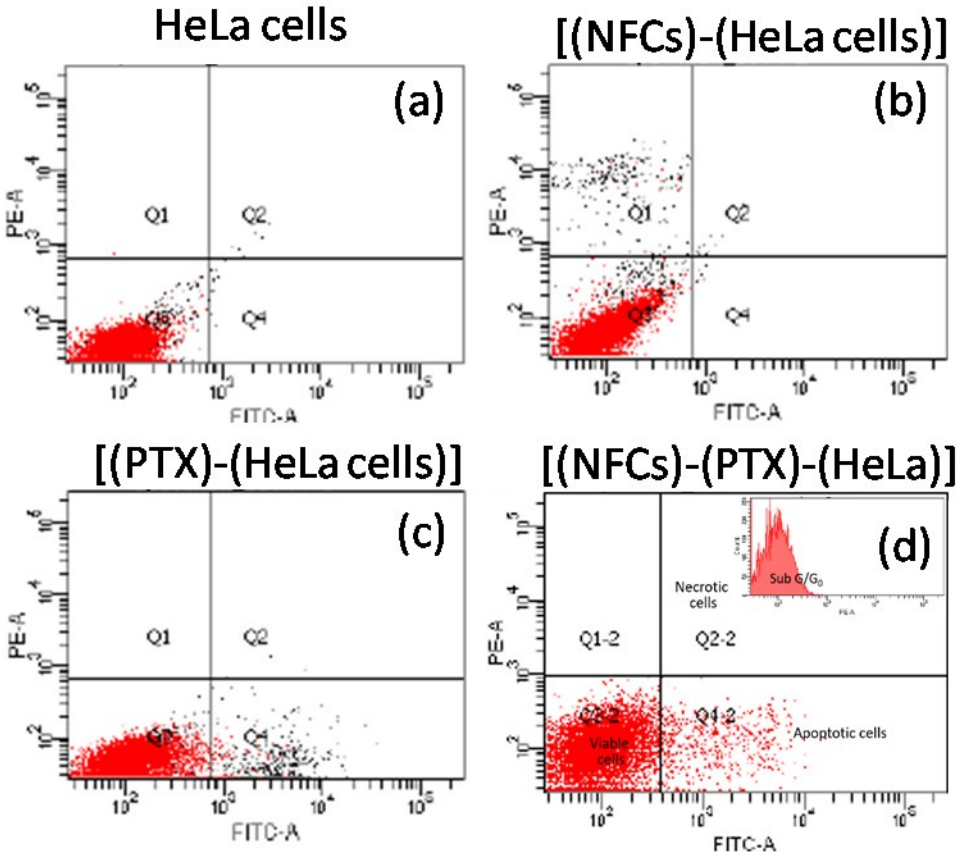

Figure: S16. FACS for cell apoptosis for HeLa cells as cultured and along with NFC, PTX and developed nanoformulation.